buildings

MDPI

Article

Multi-Objective Optimization of Sustainable Concrete Containing Fly Ash Based on Environmental and Mechanical Considerations

Kennedy C. Onyelowe [1,2,*], Denise-Penelope N. Kontoni [3,4,*], Ahmed M. Ebid [5], Farshad Dabbaghi [6], Atefeh Soleymani [7], Hashem Jahangir [8] and Moncef L. Nehdi [9]

1 Department of Civil Engineering, Michael Okpara University of Agriculture, Umudike, Umuahia 440109, Abia State, Nigeria
2 Department of Civil and Mechanical Engineering, Kampala International University, Kampala 10417, Uganda
3 Department of Civil Engineering, School of Engineering, University of the Peloponnese, GR-26334 Patras, Greece
4 School of Science and Technology, Hellenic Open University, GR-26335 Patras, Greece
5 Department of Structural Engineering, Future University in Egypt, New Cairo 11845, Egypt; ahmed.abdelkhaleq@fue.edu.eg
6 Department of Civil Engineering, Babol Norshivani University of Technology, Babol 47148-71167, Iran; farshad.dabbaghi95@gmail.com
7 Department of Civil Engineering, Shahid Bahonar University of Kerman, Kerman 7616913439, Iran; atefeh_soleymani@eng.uk.ac.ir
8 Department of Civil Engineering, University of Birjand, Birjand 9717434765, Iran; h.jahangir@birjand.ac.ir
9 Department of Civil Engineering, McMaster University, Hamilton, ON L8S 4L8, Canada; nehdim@mcmaster.ca
* Correspondence: kennedychibuzor@kiu.ac.ug (K.C.O.); kontoni@uop.gr (D.-P.N.K.)

Abstract: Infrastructure design, construction and development experts are making frantic efforts to overcome the overbearing effects of greenhouse gas emissions resulting from the continued dependence on the utilization of conventional cement as a construction material on our planet. The amount of CO_2 emitted during cement production, transportation to construction sites, and handling during construction activities to produce concrete is alarming. The present research work is focused on proposing intelligent models for fly ash (FA)-based concrete comprising cement, fine and coarse aggregates (FAg and CAg), FA, and water as mix constituents based on environmental impact (P) considerations in an attempt to foster healthier and greener concrete production and aid the environment. FA as a construction material is discharged as a waste material from power plants in large amounts across the world. Its utilization as a supplementary cement ensures a sustainable waste management mechanism and is beneficial for the environment too; hence, this research work is a multi-objective exercise. Intelligent models are proposed for multiple concrete mixes utilizing FA as a replacement for cement to predict 28-day concrete compressive strength and life cycle assessment (LCA) for cement with FA. The data collected show that the concrete mixes with a higher amount of FA had a lesser impact on the environment, while the environmental impact was higher for those mixes with a higher amount of cement. The models which utilized the learning abilities of ANN (-BP, -GRG, and -GA), GP and EPR showed great speed and robustness with R^2 performance indices (SSE) of 0.986 (5.1), 0.983 (5.8), 0.974 (7.0), 0.78 (19.1), and 0.957 (10.1) for Fc, respectively, and 0.994 (2.2), 0.999 (0.8), 0.999 (1.0), 0.999 (0.8), and 1.00 (0.4) for P, respectively. Overall, this shows that ANN-BP outclassed the rest in performance in predicting Fc, while EPR outclassed the others in predicting P. Relative importance analyses conducted on the constituent materials showed that FA had relatively good importance in the concrete mixes. However, closed-form model equations are proposed to optimize the amount of FA and cement that will provide the needed strength levels without jeopardizing the health of the environment.

Citation: Onyelowe, K.C.; Kontoni, D.-P.N.; Ebid, A.M.; Dabbaghi, F.; Soleymani, A.; Jahangir, H.; Nehdi, M.L. Multi-Objective Optimization of Sustainable Concrete Containing Fly Ash Based on Environmental and Mechanical Considerations. *Buildings* **2022**, *12*, 948. https://doi.org/10.3390/buildings12070948

Academic Editor: Marco Di Ludovico

Received: 14 June 2022
Accepted: 29 June 2022
Published: 4 July 2022

Keywords: green concrete; fly ash (FA); sustainable construction materials; life cycle assessment (LCA); environmental impact (EI); artificial intelligence (AI)

1. Introduction

1.1. Fly Ash

Substantial research has been conducted to evaluate using various supplementary cementitious materials (SCMs) such as fly ash (FA), slag, metakaolin, rice husk ash (RHA), silica fume (SF), and natural pozzolan for the partial replacement of Portland cement, which releases remarkable quantities of CO_2 [1–4]. Almost 7% of global anthropogenic greenhouse gas emissions originate from cement manufacturing [5–8]. Coal combustion for energy production is the primary industrial process for generating FA. The reduction in cement consumption, as well as eliminating fly ash disposal costs and environmental risk, are the most striking bonuses of FA use in concrete [9]. Pozzolanic activity, low water demand, reduced bleeding, and lesser heat evolution are some of the reasons why FA has been widely adopted in the construction industry as a binder replacement [10–12]. While fly ash continues to be produced in large volumes, especially in large cement-producing countries such as China and India, other countries in Europe and North America have discontinued coal-fired power plants for environmental considerations. In such countries, the use of fly ash continues through beneficiating old fly ash deposits, including in landfills.

The amorphous silica in FA undergoes a chemical reaction with calcium hydroxide during cement hydration and generates additional calcium silicate hydrate, further enhancing its mechanical properties and durability [13–16]. Various studies have demonstrated that the strength increment of FA continues for a longer period of time compared to ordinary concrete, owing to pozzolanic reactions [17]. Hence, FA can improve the long-term compressive strength of different types of concrete [18,19]. From a microstructural point of view, FA concrete specimens after early-age curing exhibit a copious amount of un-hydrated spherical FA particles. Therefore, low compressive strength has been reported during the initial stages of curing. Conversely, un-hydrated FA particles are less present after long-term curing. Hence, the microstructure of concrete incorporating FA becomes denser in the long term [20]. Deign codes such as ACI 211 [21] indicate that replacing 15% to 25% of cement with FA in high-strength concrete could be an optimum dosage. The particle size of FA is another key factor that affects the compressive strength of concrete. It has been reported that higher compressive strength was attained in concrete containing FA composed of a finer particle size distribution, compared to that of ordinary FA [22]. In addition to compressive strength, FA fineness has a significant effect on the shrinkage of concrete. In concrete incorporating coarse FA, much lower drying shrinkage was reported [23]. It has been posited that a 50% substitution of FA with OPC results in a 30% decrease in shrinkage compared to typical concrete [24]. FA also affects the porosity and transport mechanisms in concrete. For instance, Supit and Shaikh [25] depicted that FA presence in concrete mitigated the amount of permeable voids by 6 to 11% compared to that in concrete containing OPC. Ravina and Mehta [26] studied the effects of FA on the properties of concrete made with FA in the range of 35 to 50%. They reported that the mixing water required for a certain slump was reduced by 5 to 10% for concrete incorporating FA. A mercury intrusion porosimetry test confirmed that FA promoted the density of the cementitious matrix. The paste–aggregate interfacial bond in the concrete is also enhanced by FA. Conversely, Mardani-Aghabaglou et al. [27] reported that concrete samples including FA had much higher permeable voids when compared to OPC counterparts. It has been stated that the void content could be increased by increasing the FA cement replacement level in the mixture [28,29].

Sorptivity is also reduced by incorporating FA in concrete. It was found that FA addition decreased the permeability of both cement paste and the transition zone around the aggregates. Several studies have been conducted on the effects of class F FA on the

compressive strength of concrete. It has been indicated that compressive strength is reduced with the increment of FA content in concrete, as class F FA contains a small quantity of lime. However, compressive strength is boosted at later phases of curing as a result of pozzolanic activity [30–33]. Chloride ion penetrability in concrete can be notably decreased by class F FA. Wang et al. [34] have expressed that class F fly ash is highly effective at lessening chloride ion penetrability owing to its micro-filler effect and pozzolanic activity. The influence of various replacement levels of FA on the chloride ion penetrability of concrete was investigated by Chindaprasirt et al. [22] using three different test setups. In all test procedures, as the amount of FA in the concrete increased, the chloride ion penetrability in the concrete remarkably decreased.

Moreover, the source and type of FA could be another influential factor that affects the mechanical properties of concrete. For instance, high-early compressive strength could be achieved by high calcium FA compared to low calcium FA [35]. As reported by Malhotra [36], compressive strength growth differs with variation in FA content, and this is not consistent with the amorphous silica percentage; FA with high silica content results in a slower strength increase in comparison with its counterparts.

1.2. Optimization Method

Kate et al. [37] evaluated and optimized the long-term mechanical characteristics of concrete reinforced with crimped steel fibers. Multiple regression analysis was used to examine the extent of FA influence on the mechanical characteristics of concrete. It was claimed that the Taguchi methodology was an efficient strategy for reducing the total amount of exploratory research. It was also mentioned that the mechanical properties of high-strength, high-volume FA in steel-fiber-reinforced concrete offer an alternative sustainable option for the concrete industry. In another study, the optimization of the mixture proportions of green and sustainable concretes was accomplished [38]. In this respect, the model to be optimized took concrete effect into account, as well as the unit cost and environmental impact. As a result, a novel prediction technique dubbed "Marine predator programming" was developed to model and anticipate certain functional features. Three forecasting strategies were used to evaluate the effectiveness of the introduced machine learning model: artificial neural networks, support vector machines, and second polynomial regression. As a result, an innovative sustainable model was developed, and mixture components of sustainable and green concrete types for various compressive strength classes were designed. The findings suggest that marine predator programming is highly capable of estimating a variety of tangible properties. Green mixtures lessened the environmental index by 74.37% and 67.83%.

1.3. Environmental Evaluation

In recent decades, a myriad of research has been performed to mitigate the adverse effects of using OPC in concrete. The most utilitarian method to understand the impact of different SCMs on the environment is life cycle assessment (LCA). LCA is remarkable in modeling the complex process of manufacturing concrete based on environmental considerations [39,40]. Multifunctional processes are among the most challenging problems in LCA [41]. Specifically, the production of electricity and FA from coal combustion cannot be considered independently, and is a rather multifunctional process [42]. This distribution of environmental impact is known as 'allocation'. The findings of this allocation may then be engaged in the evaluation of the environmental performance of FA later in its life cycle, such as when it is mixed into concrete. The evaluation of environmental impact corresponding to product stage was investigated by Chen et al. [43]. In this research, no allocation procedure was performed for products of waste status. On the other hand, economic ratio allocation approaches were applied for products of by-product status. It is noteworthy that because of the importance of replacing OPC with different SCMs, numerous LCA studies have been conducted on concrete incorporating FA [41–45]. Using FA in concrete makes use of such a waste product and substitutes OPC in concrete, both

of which are beneficial to the environment. It is generally known that a reduction in the amount of OPC used in concrete could indeed boost the overall environmental efficiency of mix designs since, by far, OPC is the ingredient which has the greatest environmental impact [46]. From a greenhouse gas emission point of view, it has been demonstrated that replacing OPC with FA is environmentally lucrative when the distance between coal and cement plants is notably large [47]. Taking these key aspects into account, increased OPC replacement with FA has significant environmentally positive impacts.

1.4. Research Significance

With the colossal global growth of greenhouse gas (GHG) emissions, polar ice caps have been melting rapidly in the Antarctic and Arctic, extreme weather events have inflicted economic damage, and climate change effects have been accelerating. The cement and concrete industry contributes substantial GHG emissions [48,49]. Demand for concrete continues to grow worldwide. The concrete ingredient that contributes the most to GHG is Portland cement (PC). It is estimated that, by 2050, the consumption of cement will grow from the current 4.2 to 5.2 billion tons [50,51]. Using the present techniques of cement production, about 850 kg of CO_2 is released into the atmosphere per each ton of clinker produced [52]. Thus, alternative materials are needed for replacing cement to decrease the negative effect of concrete production. Using recycled material or wastes in concrete could alleviate its environmental footprint. Using supplementary cementitious materials (SCMs) is a promising solution to decrease PC consumption while disposing of waste materials from diverse industries [53–55]. SCMs have been a primary focus for enhancing concrete sustainability [56,57]. Agricultural wastes such as palm oil fuel ash (POFA), rice husk ash (RHA), olive pomace ash (OOA), sugarcane bagasse ash (SBA), and industrial wastes such as fly ash (FA) and silica fume (SF) can be used as partial replacements for cement in sustainable concrete [58,59]. It is annually estimated that the worldwide production of fly ash surpasses 900 million tons [60], with 580 million tons produced in China [61], 43.5 million tons of contribution by the United States [62], 169.25 million tons in India [63], and 14 million tons in Australia [51]. Fly ash has been used for centuries as an ingredient in cement, but its current utilization rate is only about 53.5% [60]. Waste management can lead to a number of problems, including pollution, water shortages, and the spread of disease [51]. Over the past few years, much investigation has been carried out on the application of concrete with mineral admixtures. The reaction with pozzolan, by which FA improves the microstructure and physical properties of concrete, is usually slow, so the improvements which are given to the material properties of concrete and its microstructure are mainly reflected at later stages. As a result, the early strength of concrete with FA is lower [64]. FA is a replacement material for construction which is beneficial because of its chemical features. For instance, by using FA instead of PC in concrete production, you can reduce the amount of both PC and water needed. The result is a more robust concrete that is stronger, more durable, and has higher mechanical performance [65]. Additionally, several studies have shown that fly ash enhances the durability and workability of concrete when used in concrete. Using fly ash instead of PC induces more porosity without eroding the average pore size, according to Chindaprasirt et al. [66]. Moreover, by increasing the content of fly ash, the volume of the gel pore increases by 5.7 for 10 nm. Adding large amounts of fly ash makes it harder for chloride ions in water to penetrate into the concrete, which helps prevent corrosion [67]. A study performed by Hussain et al. [68] investigated whether fly ash concrete from high-strength samples had equivalent compressive strengths to plain concrete; fly ash concrete had greater compressive strengths than ordinary concrete. Fly ash (as a partial replacement for cement) decreases the initial strength of concrete, but after 56 to180 days, concrete strength increases considerably (after exposure to high temperatures) and concrete strength is greatly increased by using fly ash [69]. Mabibi reported [70] that concrete's resistance and chloride migration coefficient could be improved by replacement with fly ash, as could the alkali–silicon reaction, although carbonization resistance would be reduced. As for fine aggregates and cement, Liu et al. [51] investigated shrinkage in creep

and curing, compression strength, and carbon dioxide emissions from concrete containing fly ash or ground granulated blast-furnace slag (GGBS). Their proposed model accurately predicted the creep strain of concrete by including a parameter to take into account the effect of fly ash content. Various waste products were used to partially replace sand and cement in Garg et al.'s study [71]. They proposed a model for predicting the compressive strength of concrete made up of fly ash and slag using an adaptive fuzzy logic model. SCC was used in Zhao et al.'s study, which employed FA at five levels (0, 20, 30, 40, and 50 percent) [72]. The mechanical properties and water porosity of the FA series SCCs, as well as their transportation properties, were investigated.

In this research work, intelligent models are proposed using three different operative algorithms—ANN (GA, GRG and BP), genetic programming (GP), and evolutionary polynomial regression (EPR)—to test the compressive strength of 28-day-cured concrete containing fly ash (FA) based on environmental impact assessment considerations for minimizing global warming potential (GWP) effects. Figure 1 presents the structural and environmental benefits of adding FA as a supplementary cement in concrete, and shows the primary focus of this research work.

Figure 1. The multiple structural and environmental benefits of FA in sustainable concrete.

2. Research Methodology

2.1. Data Collection

The extensive literature search conducted for the present research work showed that fly ash (FA) has been studied for its potential as an alternative and/or partial replacement for cement in the fight against global warming resulting from the production, transportation, and utilization of cement. The mission to save our planet from the plaguing greenhouse gas emissions (GHGE) emanating majorly from PC is in top gear, and one of those steps has been to gradually eliminate the use of PC in concrete production and construction activities entirely. Results from recent research works on the utilization of fly ash in concrete production [73–85] were gathered, and multiple data were collected, tabulated, and utilized

to propose intelligent predictions for a design, production, and performance evaluation of FA-based concrete.

2.2. Collected Database and Statistical Analysis

At the end of the literature search, 112 records were collected from experimental tested concrete mixtures with different component ratios. Each record contained the following data: water content (W) kg/m^3, cement content (C) kg/m^3, fly ash content (FA) kg/m^3, fine aggregate (sand) content (FAg) kg/m^3, coarse aggregate content (CAg) kg/m^3, 28-day cylinder compressive strength of the concrete (Fc28) MPa, and environmental impact factor (P). The collected records were divided into a training set (90 records) and a validation set (22 records). Table 1 includes the complete dataset, while Tables 2 and 3 summarize their statistical characteristics and the Pearson correlation matrix. Table 2 presents the minimum (Min) and maximum (Max) values of the studied data against the parameters of the 28-day-cured FA-based concrete. The average (Avg), the standard deviation (SD), and variance (Var) of the data are also presented in Table 2. These are presented for the training sets and validation sets. Table 3 shows how consistently correlated the input parameters are with the concrete strength (Fc) and environmental impact factors (P). Cement also showed a higher and more consistent correlation with the outputs (Fc and P) than any other parameter in the study. However, intelligent models are being proposed to optimize the consistency and relationship between FA and the outputs (Fc and P). Achieving this would achieve the optimal utilization of FA in the place of PC (C) to attain a safer environment and minimize the impact of concrete production and construction activities on the environment (P). Finally, Figure 2 shows the histograms for both inputs and outputs. While the studied input parameters showed a unimodal distribution of data, FAg and CAg showed a bimodal unsymmetrical distribution. Meanwhile, the output variables Fc and P showed unimodal unsymmetrical data distribution. In the Fc28 data distribution, it appears that the concrete strength in the 40MPa and 50MPa bin had the highest frequency, while in the P data distribution, the environmental impact % of 7 to 9 had the highest frequency. Meanwhile, Fc28 seems to partially skew towards the left.

Table 1. Utilized database.

W	C	FA	Fag	Cag	Fc28	P
kg/m^3	kg/m^3	kg/m^3	kg/m^3	kg/m^3	MPa	-
Training dataset						
171.58	199.19	85.79	388.65	835.47	34.5	5.3
202.16	459.46	68.92	326.13	713.03	42.5	9.5
220.48	237.29	34.60	770.12	352.57	27.1	4.9
252.37	283.79	167.24	667.68	305.88	33.6	8.3
233.76	477.06	71.56	383.18	585.98	36.9	9.8
150.14	101.71	101.71	542.80	754.80	8.5	4.0
196.07	435.71	65.36	295.71	771.13	41.1	9.0
155.22	168.32	147.16	357.72	879.94	25.4	6.0
161.46	322.92	107.64	376.63	785.04	41.7	7.9
172.12	278.58	119.39	335.14	828.50	53.0	7.4
160.62	160.62	160.62	364.24	860.37	33.0	6.1
258.82	324.80	187.77	637.66	292.24	39.5	9.4
154.59	107.41	146.56	386.88	884.30	13.4	5.0
162.20	226.28	226.28	320.43	831.12	48.0	8.5
223.88	238.81	59.70	756.47	346.29	29.2	5.5
146.40	385.27	96.32	216.44	952.93	27.7	8.8
242.48	538.85	80.83	365.71	549.76	42.0	11.0
154.46	94.28	146.44	395.32	882.93	10.5	4.7
220.25	199.32	64.78	773.17	354.07	22.9	4.9
171.55	239.98	103.13	372.31	820.54	45.5	6.4
161.67	425.45	47.27	212.46	935.37	38.2	8.5

Table 1. *Cont.*

W	C	FA	Fag	Cag	Fc28	P
kg/m^3	kg/m^3	kg/m^3	kg/m^3	kg/m^3	MPa	-
Training dataset						
257.16	234.58	234.58	390.51	581.41	20.9	8.8
171.55	239.98	103.13	372.31	820.54	47.0	6.4
150.94	131.47	68.17	545.71	752.41	11.9	3.8
171.58	199.19	85.79	388.65	835.47	33.5	5.3
173.01	286.71	88.98	518.31	645.04	43.7	6.9
213.26	197.47	29.62	794.88	363.82	21.3	4.2
290.79	379.62	67.32	372.02	554.49	19.9	8.0
178.50	311.39	54.54	348.25	821.22	50.0	6.7
200.55	435.97	65.40	333.89	722.64	40.7	9.0
198.28	450.64	67.60	319.87	732.08	43.6	9.3
150.99	116.89	87.67	545.87	749.42	7.4	4.0
150.70	102.09	102.09	544.84	751.22	5.8	4.0
244.25	321.65	105.54	685.94	313.97	42.5	7.8
125.31	250.63	205.06	379.92	830.85	35.6	8.6
252.27	390.92	69.33	383.09	602.78	32.0	8.3
199.96	425.45	63.82	339.08	724.87	38.9	8.8
154.76	125.62	146.72	377.93	883.29	17.1	5.3
225.86	513.31	77.00	338.79	623.73	43.9	10.5
237.33	241.35	120.68	717.57	328.73	28.5	6.7
232.81	200.70	115.40	739.77	338.63	20.0	5.9
151.80	132.21	68.55	545.76	750.22	8.8	3.9
231.42	279.30	69.82	729.15	333.97	35.6	6.3
105.59	211.17	258.10	381.99	855.63	24.0	8.9
203.96	485.63	72.84	317.49	702.32	48.4	10.0
216.33	240.48	240.48	400.33	635.89	38.8	9.0
230.38	548.51	82.28	324.45	608.54	47.9	11.2
232.71	484.81	72.72	380.34	585.88	37.7	9.9
202.29	430.41	64.56	334.99	721.96	40.3	8.9
249.55	323.31	136.39	668.08	305.58	42.7	8.4
130.56	343.57	147.24	220.58	971.16	22.5	9.0
253.69	347.61	115.22	385.24	596.58	30.3	8.4
241.52	281.77	120.76	698.01	319.65	36.5	7.4
297.03	228.26	228.26	379.99	529.80	16.6	8.6
196.93	468.88	70.33	286.11	758.61	46.1	9.7
138.68	118.87	178.30	496.49	771.89	10.1	5.8
234.12	508.97	76.35	370.78	578.11	40.3	10.4
149.86	116.02	87.01	544.79	753.39	10.4	3.9
154.36	83.19	146.34	401.91	882.33	8.4	4.5
254.63	324.62	162.31	651.85	298.78	41.2	8.9
247.22	282.53	141.27	683.56	313.19	35.5	7.8
217.32	198.47	49.62	782.23	358.46	22.4	4.6
161.60	195.52	195.52	358.39	826.09	41.5	7.4
196.93	468.88	70.33	286.11	758.61	47.3	9.7
229.22	200.20	100.10	749.77	343.07	21.4	5.6
242.07	242.07	141.21	704.62	322.38	26.9	7.1
198.88	405.87	60.88	346.21	731.71	37.2	8.4
214.66	310.50	166.73	397.23	644.16	45.0	8.8
172.12	278.58	119.39	335.14	828.50	50.5	7.4
225.59	479.99	72.00	349.67	633.94	39.9	9.9
202.16	459.46	68.92	326.13	713.03	43.1	9.5
235.58	318.08	49.70	717.32	328.87	39.3	6.6
294.42	294.42	158.10	376.65	540.14	19.9	8.3
138.68	118.87	178.30	496.49	771.89	9.6	5.8
227.80	277.32	39.62	744.96	341.42	33.0	5.7
231.63	454.17	68.13	393.07	593.85	35.2	9.3
223.69	199.72	84.88	761.67	348.85	22.7	5.3

Table 1. *Cont.*

W	C	FA	Fag	Cag	Fc28	P
kg/m^3	kg/m^3	kg/m^3	kg/m^3	kg/m^3	MPa	-
Training dataset						
178.19	222.50	39.38	400.28	824.38	33.0	4.8
231.14	240.15	100.06	732.67	335.68	29.8	6.3
227.94	239.94	79.98	743.87	340.67	29.6	5.9
155.62	131.30	68.08	542.01	748.28	9.6	3.8
203.96	485.63	72.84	317.49	702.32	47.3	10.0
212.44	401.17	71.14	393.13	655.13	47.4	8.5
172.12	278.58	119.39	335.14	828.50	50.5	7.4
150.70	102.09	102.09	544.84	751.22	6.1	4.0
195.08	433.52	65.03	296.92	772.97	39.0	8.9
151.27	117.11	87.84	543.86	750.84	7.9	4.0
292.59	337.75	111.96	374.32	547.36	21.0	8.2
199.96	425.45	63.82	339.08	724.87	38.4	8.8
240.49	320.65	80.16	700.02	320.27	41.4	7.3
Validation dataset						
171.55	239.98	103.13	372.31	820.54	49.5	6.4
150.94	131.47	68.17	545.71	752.41	12.5	3.8
224.52	510.27	76.54	339.96	626.77	43.2	10.5
171.58	199.19	85.79	388.65	835.47	33.5	5.3
122.64	126.87	296.02	394.96	837.80	30.6	8.2
178.12	356.23	62.86	374.87	764.13	48.9	7.6
236.72	280.86	95.29	713.23	326.56	36.2	6.9
146.87	132.18	137.08	506.00	762.97	13.1	5.2
255.12	302.83	162.61	387.42	590.31	32.7	8.6
146.87	132.18	137.08	506.00	762.97	11.2	5.2
196.98	198.87	56.82	574.90	609.75	23.2	4.7
202.29	430.41	64.56	334.99	721.96	39.6	8.9
196.57	446.75	67.01	331.02	725.75	44.0	9.2
145.75	116.60	87.45	547.51	757.15	9.0	4.0
126.32	210.53	210.53	393.26	834.18	66.5	8.0
196.57	468.03	70.20	285.59	760.33	45.1	9.6
223.52	475.57	71.34	352.37	637.53	38.9	9.8
170.60	293.59	142.83	450.21	687.75	54.3	8.1
150.14	101.71	101.71	542.80	754.80	7.3	4.0
213.58	356.64	118.22	395.25	649.47	43.2	8.6
114.09	300.23	200.15	224.89	990.10	21.6	9.3
177.96	267.93	47.46	390.90	805.02	44.5	5.8

Table 2. Statistical analysis of collected FA–concrete database.

	W	C	FA	FAg	CAg	Fc28	P
	kg/m^3	kg/m^3	kg/m^3	kg/m^3	kg/m^3	MPa	-
Training set							
Min.	105.6	83.2	29.6	212.5	292.2	5.8	3.8
Max.	297.0	548.5	258.1	794.9	971.2	53.0	11.2
Avg.	201.1	292.7	105.2	469.7	635.1	31.7	7.3
SD	42.2	125.5	50.8	165.3	202.0	13.0	2.0
VAR	0.2	0.4	0.5	0.4	0.3	0.4	0.3
Validation set							
Min.	114.1	101.7	47.5	224.9	326.6	7.3	3.8
Max.	255.1	510.3	296.0	713.2	990.1	66.5	10.5
Avg.	178.1	276.3	111.9	425.1	727.9	34.0	7.2
SD	37.5	127.4	59.7	109.5	125.3	15.9	2.1
VAR	0.2	0.5	0.5	0.3	0.2	0.5	0.3

Table 3. Pearson correlation matrix of the FA–concrete parameters.

	W	C	FA	FAg	CAg	Fc28	P
W	1.00						
C	0.47	1.00					
FA	−0.19	−0.36	1.00				
FAg	0.29	−0.44	−0.11	1.00			
CAg	−0.78	−0.11	0.15	−0.80	1.00		
Fc28	0.23	0.68	−0.10	−0.34	−0.03	1.00	
P	0.40	0.88	0.12	−0.54	−0.03	0.68	1.00

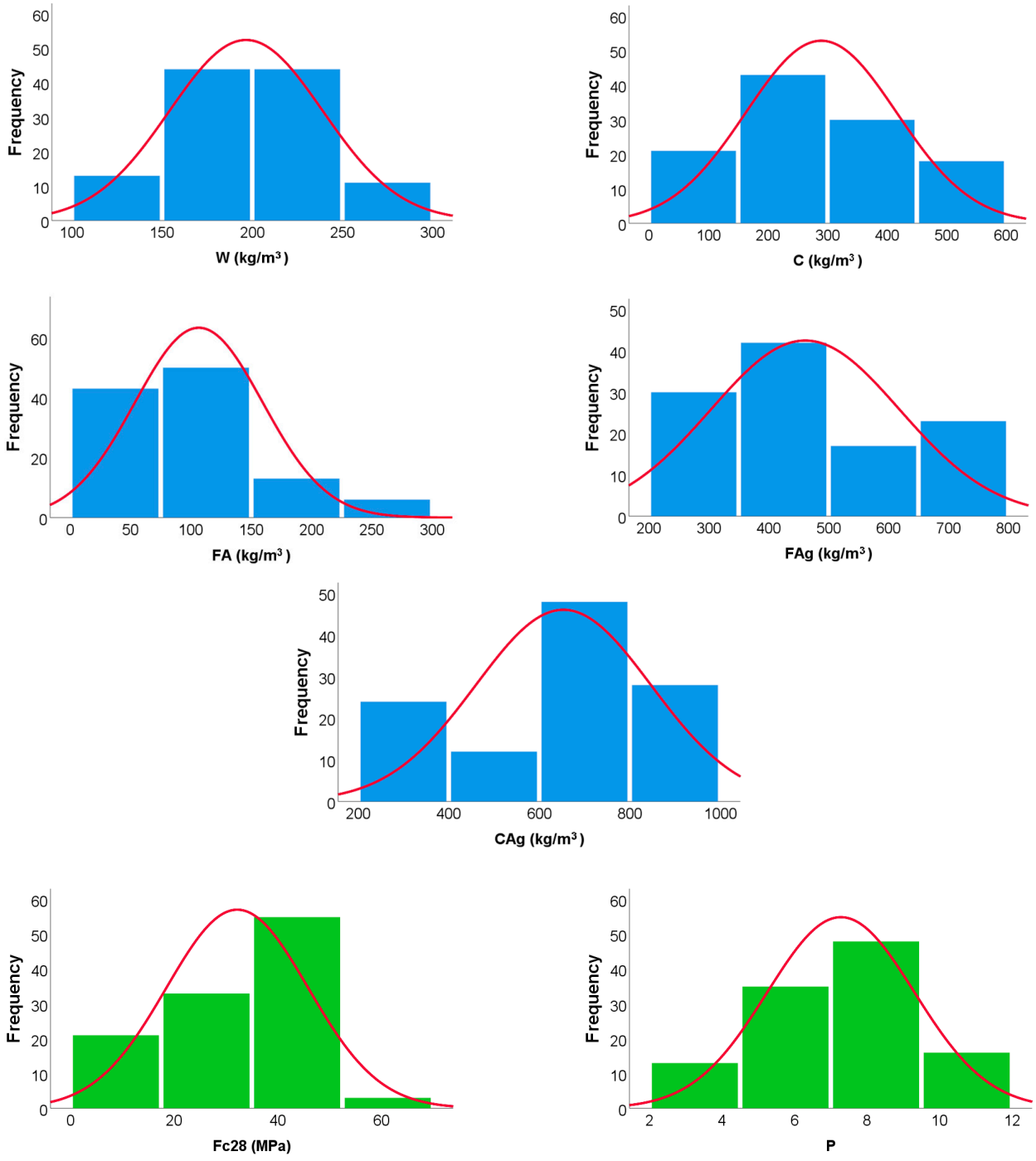

Figure 2. Distribution histograms for inputs (in blue) and outputs (in green).

2.3. Research Program and Modelling Plan

Five different artificial intelligence (AI) techniques were used to predict the confined compressive strength of the concrete short rectangular column wrapped with FRP sheets using the gathered dataset. The implemented techniques were "artificial neural network (ANN-BP, ANN-GRG and ANN-GA)", "genetic programming (GP)" and "evolutionary polynomial regression (EPR)". All these techniques were used to predict both 28-day compressive strength (Fc28, MPa) and the environmental impact factor (P) using water content (W, kg/m^3), cement content (C, kg/m^3), fly ash content (FA, kg/m^3), fine aggregate (sand) content (FAg, kg/m^3) and coarse aggregate content (CAg, kg/m^3).

Each implemented technique was based on a different approach: mimicking the human brain for ANN, the optimization of mathematical regression for EPR, and simulating the evolution of natural creatures for GP. However, for all techniques, their accuracies were evaluated in terms of the "sum of squared errors (SSE)", "root mean squared errors (RMSE)", and the "determination coefficient (R^2)".

2.3.1. Genetic Algorithm (GA)

The GA is a mathematical technique which simulates the evolution process of biological creatures [60]. It depends on one simple rule: "The most fitting creature will survive". To apply this principal on optimization, there must be a pool of solutions for the considered problem, fitting criteria, and a procedure to generate new solutions by mixing the existing ones [60]. Biological creatures transfer their data to the next generation in an arranged series of genes called "chromosomes"; similarly, the GA presents the solution (chromosome) as an arranged list of steps (genes) [60]. This allows the GA to apply genetic operations (such as crossover and mutation) to the solutions [60]. Crossover is a mixing procedure used to generate two new solutions from two existing ones by swapping the head and tails of the two existing solutions [60]. Mutation presents the random change in genetic data due to radiation, chemicals, and copying errors; it is applied by randomly changing a step of the considered solution. The algorithm cycle begins with generating a set of random solutions for the considered problem (population), evaluating the fitness of each solution using the fitting criteria, selecting the best fitting solutions and deleting the rest, and finally restoring the original population size by mixing the survival solutions (using crossover and mutation procedures) to generate new ones, and then the cycle starts again [60]. Cycle after cycle, the fitting of the solutions increases until the accepted level is reached.

2.3.2. Genetic Programming (GP)

GP is an application of the previously mentioned GA technique [60]. It depends on using the GA as a "multi-variable and structure-free regression technique", where the population is a set of randomly generated mathematical formulas and the fitting criteria is the "Sum of Squared Errors (SSE)" between the predicted values and the correct values of the training dataset [60]. In order to apply genetic operations, each solution (formula) must be presented in genetic form (as chromosome). Instead of the steps list of the GA, the chromosome consists of two parts; the first is a list of mathematical operators (=, +, −, *, /, ...) and the second one is a list of variables [60]. Crossover and mutation procedures are applied to both formula operators and variables separately to generate new formulas (solutions). Cycle after cycle, the SSE decreases, and the accuracy of the solutions (formulas) increases. Finally, the accuracy of the developed formula is tested using a new validation dataset.

2.3.3. Evolutionary Polynomial Regression (EPR)

EPR is another application of GA, and it depends on optimizing the number of terms of the "Traditional Polynomial Regression (TPR)" [60]. TPR is a well-known mathematical regression technique that uses the "Least Squared Error" principle to find the optimum coefficient values of a certain polynomial function to fit a certain dataset [60]. The considered polynomial may be single or multi-variable depending on the considered problem

configuration (dataset) [60]. The chosen polynomial degree (its highest power) depends on the complexity of the considered problem; first-degree polynomials (linear) may be used for simple problems, while for more complicated ones, second-degree (quadratic), third-degree (cubic) of higher degrees may be required [60]. The number of polynomial terms dramatically increases with increasing variable numbers and polynomial degree; for example, a two-variable second-degree polynomial has only 6 terms ($X^2 + Y^2 + XY + X + Y + C$), while a three-variable third-degree polynomial has 20 terms, and a four-variable fourth-degree polynomial has 70 terms, and so on [60]. As the number of polynomial terms increases, it becomes more difficult to apply them less practically. Hence, the EPR technique aims to optimize the TPR by eliminating the less important terms and keeping only the most effective ones using the GA technique [60]. Thus, the population (solutions) consists of a set of polynomials, the fitting criteria is the "Sum of Squared Errors (SSE)", the chromosome consists of a list of polynomial terms, and the length of the chromosome is the chosen number of terms. Cycle after cycle, the most important terms accumulate in the survival chromosomes, and the less important ones are deleted.

2.3.4. Artificial Neural Network (ANN)

The ANN is an umbrella of a wide range of AI techniques that depend on mimicking the behavior of biological neurons [60]. They all consist of nodes (cells or neurons) and link to connect the nodes, but they have different neuron arrangements and connection patterns [60]. "Multi-Layer Perceptron (MLP)" is one of the earliest and most common ANN type. It is the commonly used type for regression problems [60]. It consists of a number of nodes arranged in layers; the first layer is called the "Input layer", and it is used to receive the input values, while the last layer is called the "Output layer", and it is used to deliver outputs values [60]. Between the input and the output layers, there are a number of intermediate layers called "Hidden layers" which are responsible for predicting the outputs from the inputs. MLP must have one hidden layer at least. Each node in a certain layer is connected to all the nodes in the previous and the next layers by links, but the nodes of each layer are not connected to each other [60]. Each link has an importance factor called "Weight", and each node has a triggering formula called "Activation Function", this could be any nonlinear function, but the most popular ones are the sigmoid, the hyper-tan, and the ramp functions, which are responsible for the nonlinear capability of the ANN [60]. Due to the variation in ranges of input values, all inputs must be scaled to a unified range; this process is called "Standardization" if the input variance is divided by its standard deviation (SD), "Normalization" if the inputs are scaled between 0 and 1, and called "Hyper normalization" if the inputs are scaled between -1 and 1. The scaled inputs propagate from the input layer to the output layer through the hidden layers. The output of a certain node is the result of applying its activation function on the summation of the node inputs multiplied by the corresponding link weights [60]. After the output layer, the outputs must be de-scaled to their original renege. Any ANN model must be trained using a given dataset; during the training process, the weight values of the model's links are adjusted to predict the correct outputs from the inputs [60]. There are many training techniques that could be used to find the optimum values for links' weights, such as "Back Propagation (BP)", the "Gradually Reduced Gradient (GRG)" and the "Genetic Algorithm (GA)".

ANN Using "Back Propagation (ANN-BP)"

BP is the earliest ANN training technique, and has become the default training technique in most ANN commercial software [60]. During the training process, the data propagate forward from the input layer to the output layer to calculate the outputs' values; then, the calculated values are compared to the correct ones from the training dataset, and the errors are back-propagated from the output layer to the input layer, which is why it is called "Back Propagation" [60]. During the back propagation, the error values are divided on the links according to their weights. The updated weights are equaled to the original weight by subtracting the share of error. BP is a sequential training technique

where the ANN weights are updated record by record [60]. This iterative process is slow, but it requires limited computational capability.

ANN Using "Gradually Reduced Gradient (ANN-GRG)"

GRG is a well-known mathematical regression technique [60]. It is used to optimize the coefficients of a certain formula to fit a certain dataset by minimizing the SSE between the predicted and the correct values of the database [60]. The technique begins with assuming random values for the coefficients of the formula, and then continues by gradually changing the values of the coefficients one by one while monitoring the SSE value [60]. If changing the value of a certain coefficient decreases the SSE value, the process continues, and if it increases the SSE value, the change is applied with the opposite sign. This cycle continues until the minimum SSE value is achieved. This technique is used to train the ANN models by considering the whole ANN as one huge and extremely complicated formula, and the links' weights are its coefficients. The GRG is used to gradually adjust the values of the weights (coefficients) to minimize the SSE of the ANN [60]. This training technique is classified as the "Batch technique" because it deals with the error of the whole dataset at once, unlike sequential procedures such as BP. Hence, it is faster than BP but requires much more computational capability to deal with the whole dataset together.

ANN Using "Genetic Algorithm (ANN-GA)"

Similar to GRG, the GA technique deals with the ANN as one huge formula that needs optimization [60]. The GA training technique begins with generating a random set of solutions; each solution is a list of ANN weights [60]. Next, the fitness of each solution (SSE) is evaluated, and the most fitting solutions are selected and used to generate new solutions (lists of weights) by applying crossover and mutation [60]. In this technique, crossover is applied at multiple points along the chromosome, not just at the middle as in the original GA technique [60]. Cycle after cycle, the model converges to the optimum list of weights. The accuracy of this technique is not as sharp as BP and GRG because the initial weight values of the randomly generated solutions are not changed during training, only the combinations of the weights are changing [60]. For example, if the initial random values of a certain weight are 0.214, 0.558 and 0.331 and the correct value is (0.472), then (0.558) will appear in the final model [60]. Although this may not be the optimum value, it is the closest available one to the optimum. However, this error could be insignificant if the random population is large enough; for example, the error of a randomly generated population of 1000 records with a uniform probability density function is 1/1000 of the weight range, which is insignificant [60]. As an AI technique, the GA is less efficient than the GRG for a problem with a limited number of variables, but as the number of variables increases, GRG becomes very complicated and requires a lot of time and computational resources, and hence GA presents a much faster and less resource-consuming technique.

2.3.5. Model Performance Assessment

The models were evaluated by using indices of performance evaluation including the coefficient of determination (R^2), the sum of squares errors, and the root mean squared error, which is embedded in Taylor's diagram. The R^2 shows how well the developed models fit the measured data. For example, an R^2 value of 0.85 shows that 85% of the studied data fit the models. Generally, the R^2 ranges between −1 and 1 on the two sides of zero (0), which shows a perfect fit, while zero shows a no fit, and literally it ranges between 0 and −1 and 0 and 1. It is statistically computed as follows:

$$R^2 = \frac{SS_{regression}}{SS_{total}} \quad (1)$$

where $SS_{regression}$ is the sum of the squares due to regression and SS_{total} is the total sum of the squares. Additionally, SSE is the measure of the discrepancy between the measured data and the estimated models. This is a commonly used statistical error measurement

previously used in recent research works. The next section presents the results of each technique and their accuracy metrics.

3. Results and Discussion

3.1. Behavior of the Concrete Mixes and Environmental Impact (EI)

It is conventional that an increase in the amount of Portland cement utilized in concrete increases its mechanical properties, including compressive strength (Fc). From the collected data in Table 1, it can be observed that our results are consistent with the known results of the increase in cement amounting to increasing strength. However, the focus of this work is on underscoring what effect the addition or replacement of cement with FA has on concrete strength and, of course, the environmental impact of this mixing process. For example, a mix ratio that recorded a relatively high compressive strength of 42.5 MPa contained 459.46 kg/m^3 of cement and 68.92 kg/m^3 of FA with an environmental impact potential (EIP or P) of 9.5%. Meanwhile, another concrete mix recorded 33.6 MPa with a cement content of 283.79 kg/m^3 and a FA content of 167.24 kg/m^3; however, it had an environmental impact potential of 8.3%. This shows a reduced impact on the environment with a higher amount of FA compared to the first mix. However, the P was still high. The mix with the lowest EIP of all the concrete mixes recorded 3.8%; the amount of cement needed to achieve this was 131.47 kg/m^3 with a fly ash content of 68.17 kg/m^3, which resulted in a compressive strength of 11.9 MPa. Thus, there is an urgent need to keep the amount of cement as low as possible in order to maintain a reduced impact (P) on the environment as well as develop a relatively high-strength concrete that meets the minimum requirements for constructed infrastructure. Certainly, from the results of the literature search [13–16], it has been observed that increased FA increases the mechanical properties of concrete due to the amorphous silica in FA, which undergoes a chemical reaction with $Ca(OH)_2$ to generate the strength-based compound of calcium silicate hydrate (CSH). However, the early-stage strength of concrete is compromised due to the delay in strength gain resulting from FA inclusion. The developed intelligent models were used to determine the optimized combinations, i.e., the minimum amount of cement and the maximum amount of FA needed to develop an FA-based concrete with the required and/or minimum strength for constructed infrastructure with the lowest amount of environmental impact.

3.2. Prediction of Compressive Strength (Fc) and Environmental Impact (P)

3.2.1. Model (1)—Using the GP Technique

The developed GP model had six levels of complexity. The population size, survivor size, and the number of generations were 250,000, 50,000, and 500, respectively. Equations (2) and (3) present the output formulas for Fc28 and P. The average errors in % of the total dataset were 19.1% and 0.8%, while the coefficient of determination (R^2) values are 0.788 and 0.999, in order.

$$\text{Fc28} = \frac{1}{11\ (0.54\ \text{X})^{\ 9.15\text{X}}}, \quad X = \left(\frac{W}{C}\right)^{0.75} \tag{2}$$

$$P = \frac{Ln(C)(C + FA)(Ln(FA) + C + 5)}{(60C.Ln(C) - 20C)} \tag{3}$$

3.2.2. Models (2, 3, and 4)—Using ANN Techniques

Three models were developed using the ANN technique. All the models had the same layout (5:7:2), normalization method (−1.0 to 1.0), and activation function (hyper-tan). However, each model utilized a different training algorithm as follows: model (2) used the traditional "Back Propagation (BP)" algorithm; model (3) used the well-known mathematical algorithm "Gradually Reduced Gradient (GRG)", and model (4) used the famous AI optimization technique of the "Genetic Algorithm (GA)".

These three developed models were used to predict Fc28 and P values. The used network layout is illustrated in Figure 3, while the weights matrixes of each model are shown in Tables 4–6. The average errors in % of the total dataset were (5.1%, 2.2%), (5.8%, 0.8%) and (7.0%, 1.0%), and the (R^2) values were (0.986, 0.994), (0.983, 0.999) and (0.974, 0.999), respectively. The relative importance values for each input parameter are illustrated in Figure 4, which indicates that cement content (C) was the most important factor, then aggregate content (FAg and CAg). Fly ash and water content came last in the importance ranking.

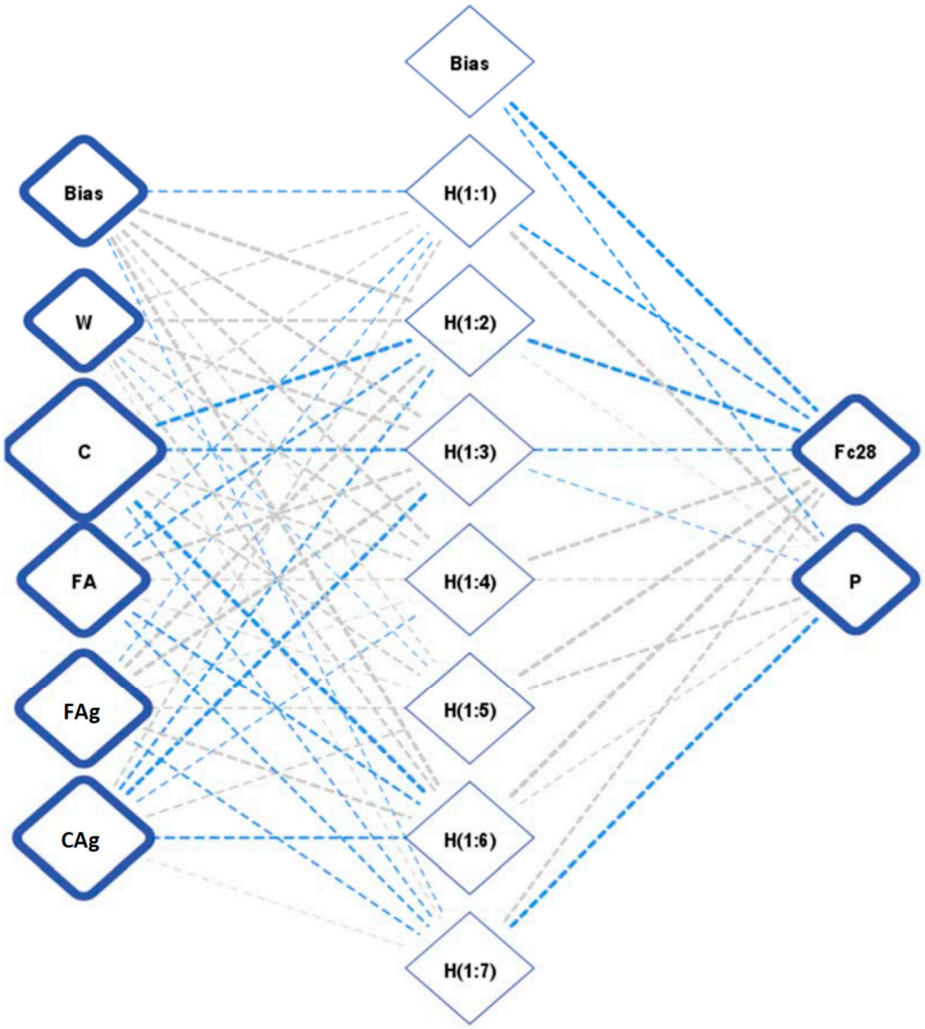

Figure 3. Architecture layout for the developed ANN models.

Table 4. Weights matrix for the developed ANN-BP model.

		Hidden Layer							
		(1–1)	(1–2)	(1–3)	(1–4)	(1–5)	(1–6)	(1–7)	
Input Layer	(Bias)	−0.20	1.95	1.47	1.09	0.14	1.86	−0.11	
	W	0.22	1.09	1.48	0.44	−0.05	0.63	0.05	
	C	0.15	−3.86	−1.37	0.45	0.38	−3.43	−0.20	
	FA	−0.16	-0.80	1.58	0.18	0.10	-0.68	−0.32	
	FAg	−0.12	1.79	3.03	0.07	0.24	1.15	−0.31	
	CAg	0.30	−0.59	−2.40	−0.14	0.27	−1.01	0.02	
		Hidden Layer							
		(1–1)	(1–2)	(1–3)	(1–4)	(1–5)	(1–6)	(1–7)	(Bias)
Output Layer	Fc28	−0.83	−2.73	−0.37	1.67	3.25	3.56	1.04	−2.04
	P	2.15	0.01	−0.11	0.13	1.05	0.15	-2.47	−0.25

Table 5. Weights matrix for the developed ANN-GRG model.

		Hidden Layer							
		(1–1)	(1–2)	(1–3)	(1–4)	(1–5)	(1–6)	(1–7)	
Input Layer	(Bias)	0.96	0.88	1.05	2.79	−0.95	0.74	−2.50	
	W	2.00	−0.89	0.17	−0.28	−1.25	0.15	1.32	
	C	−6.73	0.18	−0.76	1.52	6.05	0.44	−0.97	
	FA	−2.04	−0.44	−0.49	1.09	1.81	0.09	1.41	
	FAg	3.24	−0.08	0.29	−0.84	−2.77	−0.56	2.17	
	CAg	−0.95	0.93	0.34	−0.88	1.17	−0.47	−2.07	
		Hidden Layer							
		(1–1)	(1–2)	(1–3)	(1–4)	(1–5)	(1–6)	(1–7)	(Bias)
Output Layer	Fc28	−3.70	2.16	−0.60	−0.43	−4.52	4.12	0.89	−2.63
	P	−0.08	-0.03	−3.29	3.18	-0.08	-0.02	−0.02	−0.33

Table 6. Weights matrix for the developed ANN-GA model.

		Hidden Layer							
		(1–1)	(1–2)	(1–3)	(1–4)	(1–5)	(1–6)	(1–7)	
Input Layer	(Bias)	1.77	0.32	0.61	−0.57	0.61	−1.43	1.87	
	W	0.89	−0.18	2.78	−2.57	1.11	−4.93	4.45	
	C	−2.52	2.07	−2.30	3.37	6.53	6.68	−7.43	
	FA	−1.62	1.38	−1.34	1.46	1.08	0.61	−0.87	
	FAg	1.42	−0.14	−1.13	0.80	−1.50	-3.41	4.18	
	CAg	1.67	−0.20	1.19	−1.25	−0.27	1.31	−1.03	
		Hidden Layer							
		(1–1)	(1–2)	(1–3)	(1–4)	(1–5)	(1–6)	(1–7)	(Bias)
Output Layer	Fc28	−0.07	−1.84	2.73	2.55	2.63	3.93	4.33	−2.41
	P	−3.10	3.27	−0.08	−0.11	0.30	−0.07	−0.09	−0.18

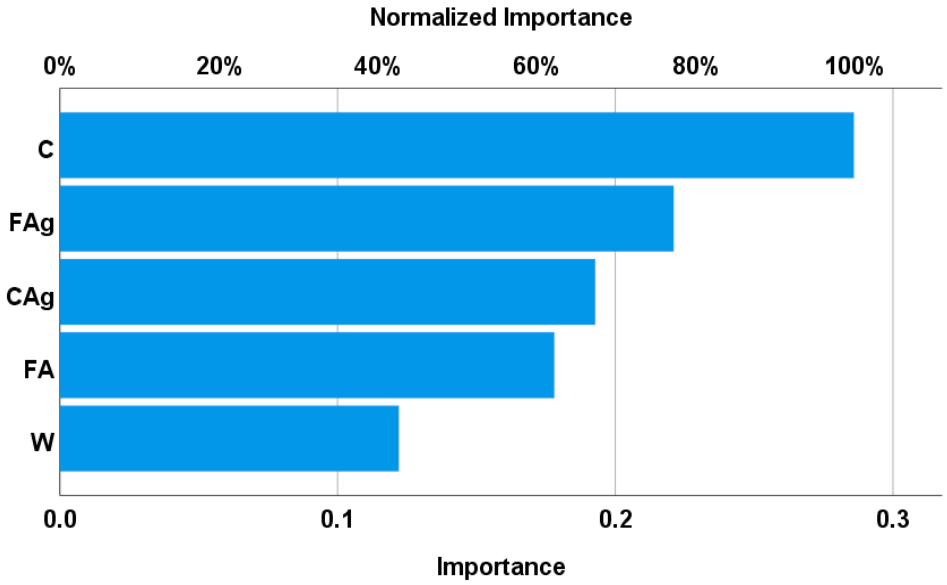

Figure 4. Relative importance of input parameters.

3.2.3. Model (5)—Using the EPR Technique

Finally, the developed EPR model was limited to the cubic level for Fc28 and the linear level for P. For 5 inputs there were 56 possible terms (35 + 15 + 5 + 1 = 56) for Fc28 and only 6 terms for P, as follows:

$$\sum_{i=1}^{i=5}\sum_{j=1}^{j=5}\sum_{k=1}^{k=5} X_i \cdot X_j \cdot X_k + \sum_{i=1}^{i=5}\sum_{j=1}^{j=5} X_i \cdot X_j + \sum_{i=1}^{i=5} X_i + C \quad (4)$$

The GA technique was applied to these polynomials to select the most effective 28 terms to predict Fc28 and 3 terms to predict P. The outputs are illustrated in Equations (5) and (6).

The average error in % and R^2 values were 10.1%—0.957 and 0.4%—1.000 for Fc28 and P, respectively. The results of all the developed models are summarized in Table 7. Figures 5–7 graphically compare the accuracies of the developed models. The relations between the calculated and predicted values are shown in Figures 8 and 9.

Table 7. Performance and accuracies of the developed models.

Item	Technique	Model	SSE	Avg. Error %	R^2
Fc28	GP	Equation (1)	4238	19.1	0.788
	ANN-BP	Figure 3, Table 3	306	5.1	0.986
	ANN-GRG	Figure 3, Table 4	392	5.8	0.983
	ANN-GA	Figure 3, Table 5	568	7.0	0.974
	EPR	Equation (3)	1195	10.1	0.957
P	GP	Equation (2)	0	0.8	0.999
	ANN-BP	Figure 3, Table 3	3	2.2	0.994
	ANN-GRG	Figure 3, Table 4	0	0.8	0.999
	ANN-GA	Figure 3, Table 5	1	1.0	0.999
	EPR	Equation (4)	0	0.4	1.000

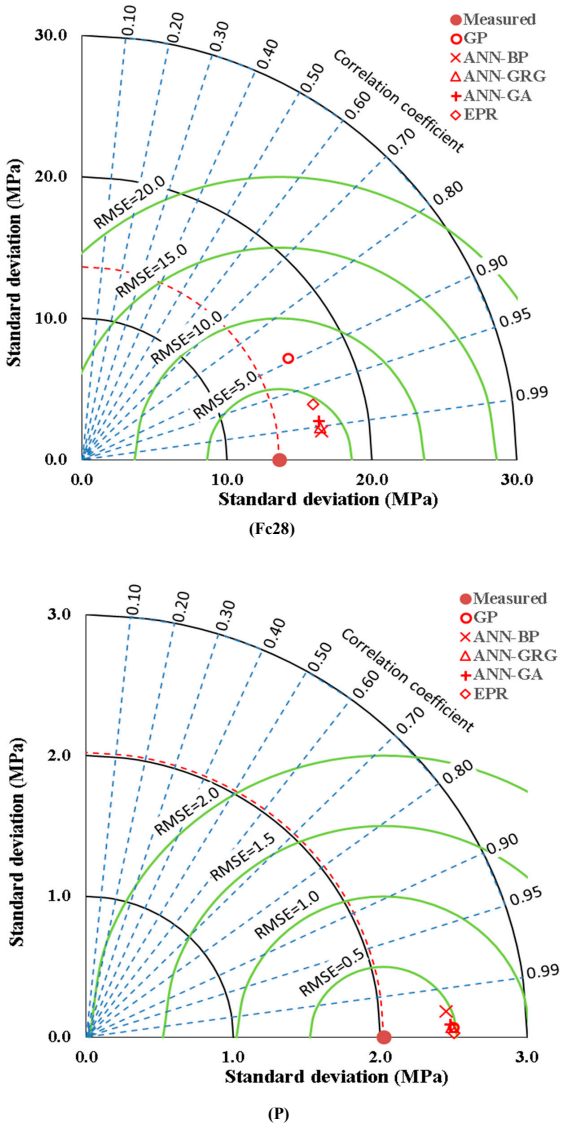

Figure 5. Comparison between developed models using the Taylor diagram for the compressive strength (Fc28) and the life cycle assessment impact point (P).

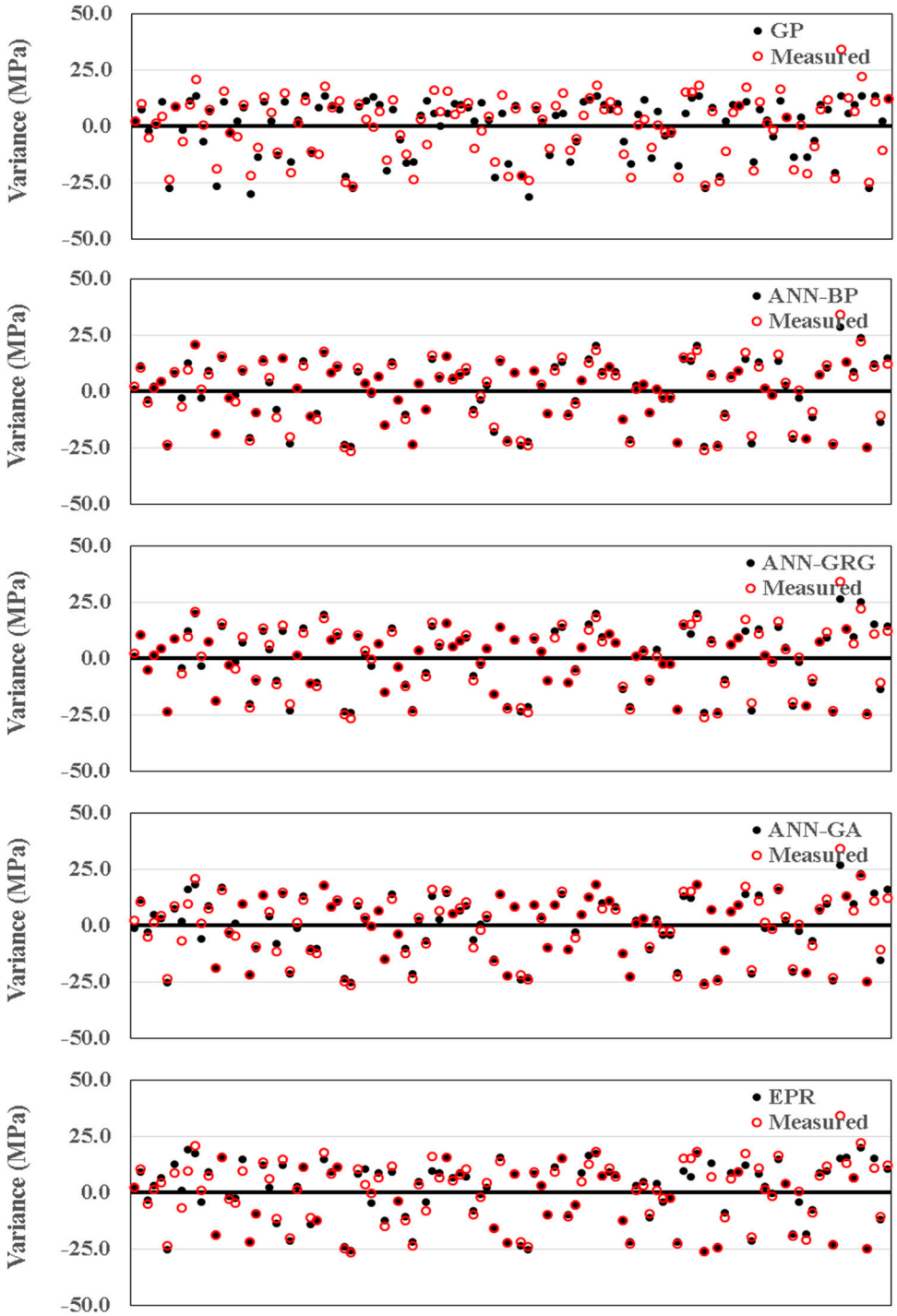

Figure 6. Comparison between developed models for Fc28 using variance diagrams.

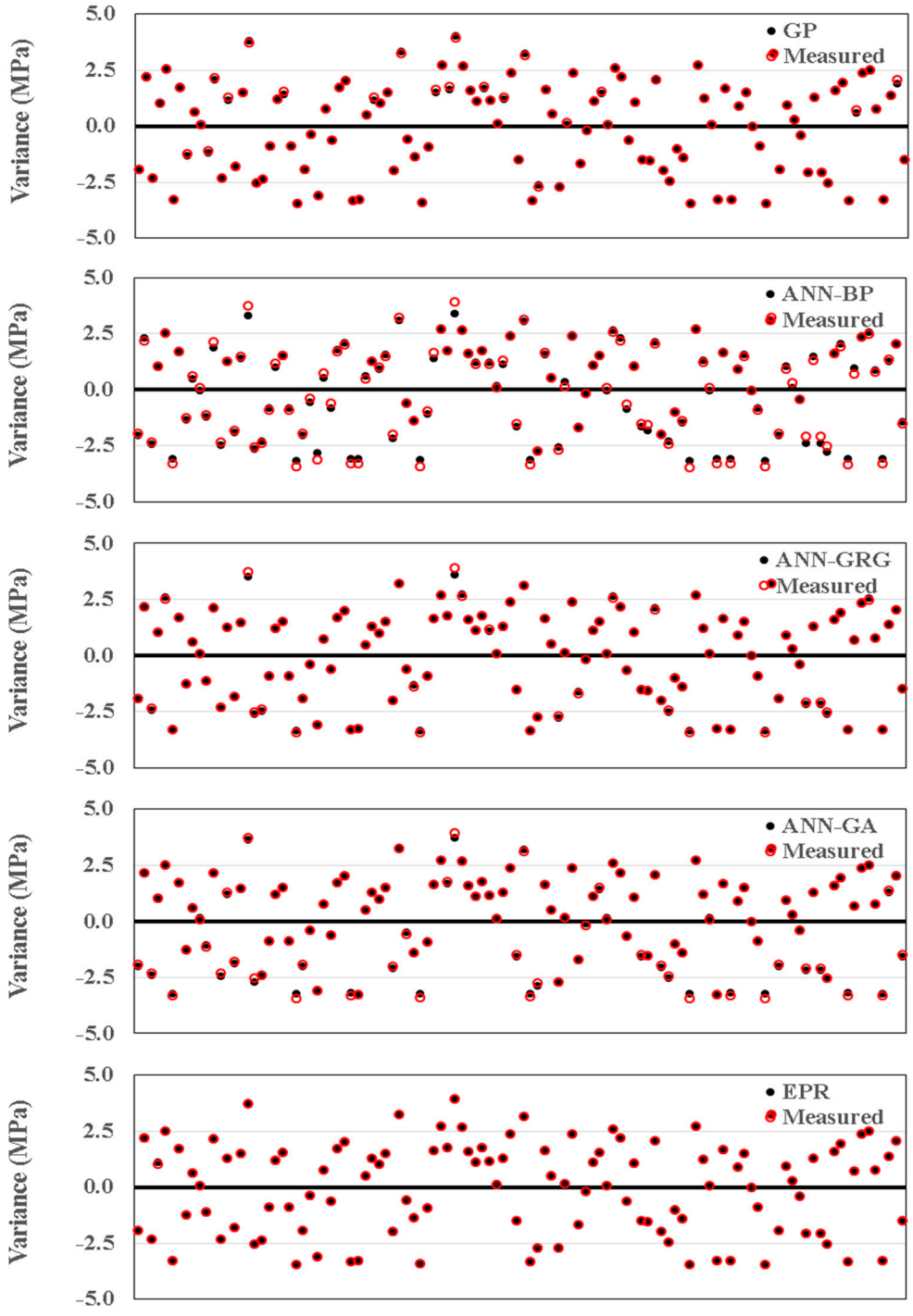

Figure 7. Comparison between developed models for P using variance diagrams.

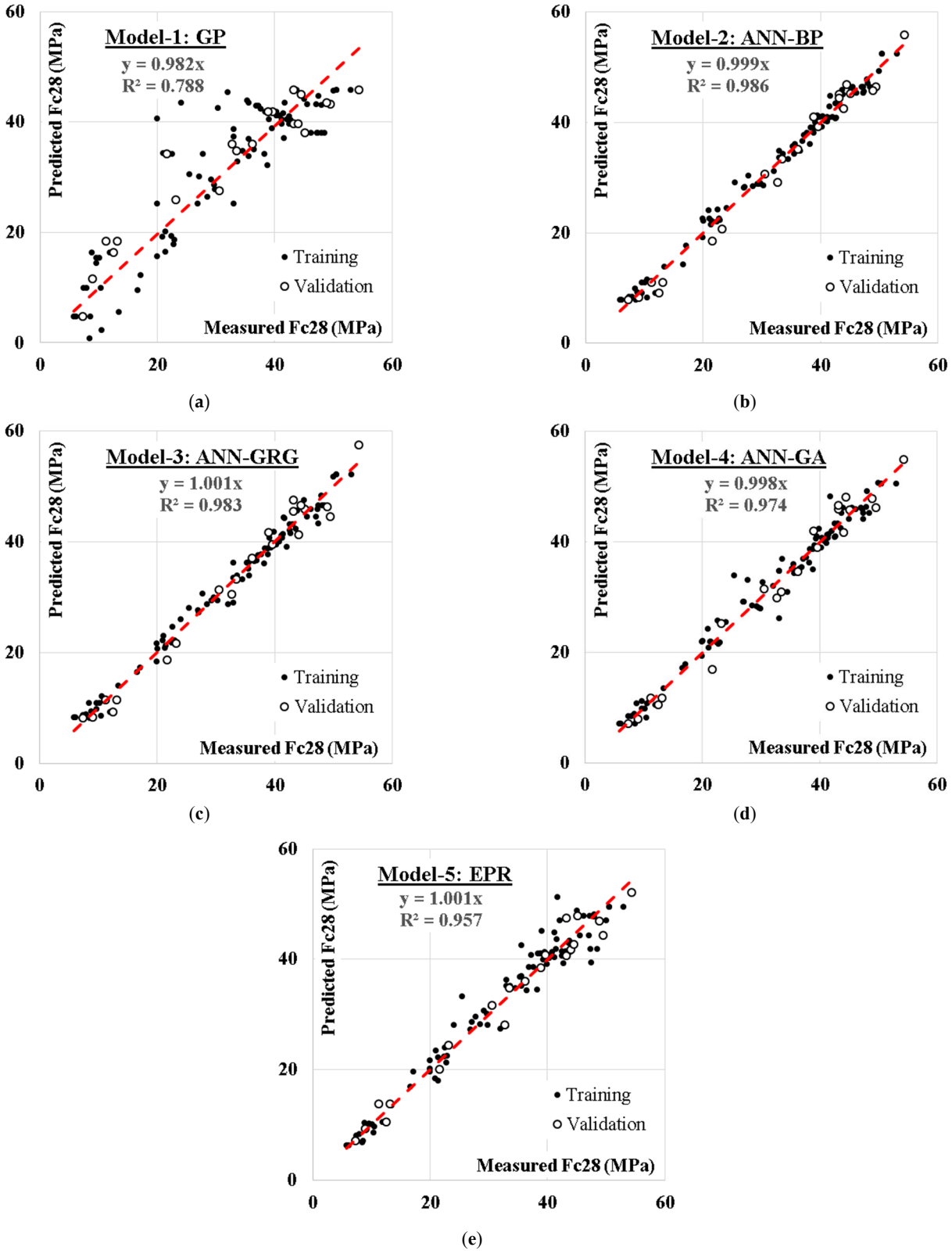

Figure 8. Relation between predicted and calculated Fc28 values using the developed models. (**a**) Model-1: GP; (**b**) Model-2: ANN-BP; (**c**) Model-3: ANN-GRG; (**d**) Model-4: ANN-GA; (**e**) Model-5: EPR.

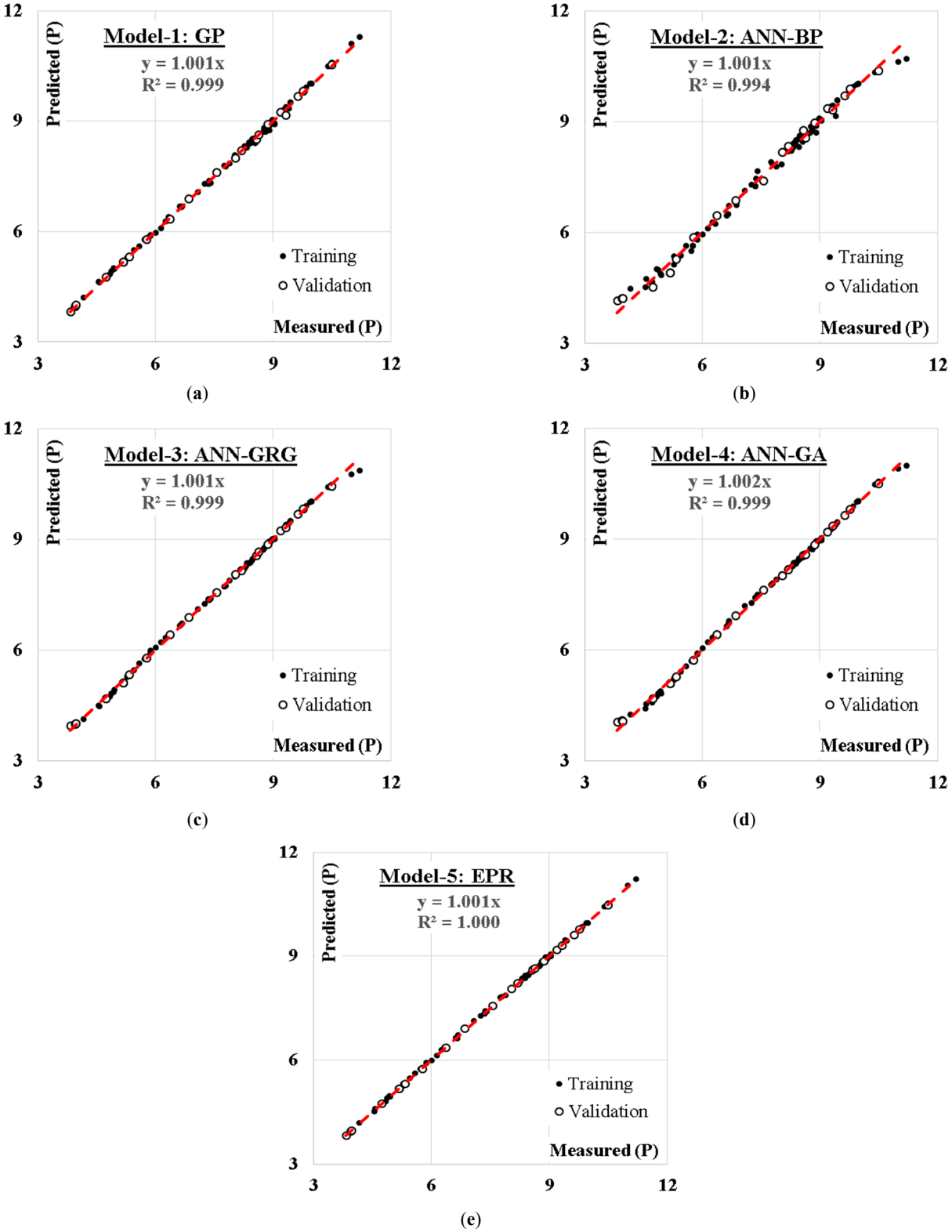

Figure 9. Relation between predicted and calculated P values using the developed models. (**a**) Model-1: GP; (**b**) Model-2: ANN-BP; (**c**) Model-3: ANN-GRG; (**d**) Model-4: ANN-GA; (**e**) Model-5: EPR.

Khursheed et al. [73] investigated predictions for the compressive strength of fly ash concrete by adopting minimax probability machine regression (MPMR), a relevance vector machine (RVM), genetic programming (GP), an emotional neural network (ENN) and

an extreme learning machine (ELM). In this research into the 28-day-cured compressive strength of concrete, it was judged that MPMR with a performance index of 0.992 was the decisive model for the forecasting of concrete strength. Meanwhile, in comparison with the model decision of Khursheed et al. [73], the present research paper used the learning abilities of ANN (BP, GRG, and GA), GP and EPR, and it has been shown that ANN-BP with a performance index of 0.986 outclassed other techniques and was adjudged the decisive technique. However, compared to the previous work [73], ANN-BP achieved 98.6% efficiency with minimal errors. Clear statistical parameters, figures of distribution, best-fit diagrams, and Taylor diagrams were used to judge the accuracy of these models. A further step has been taken in this present research work to predict the environmental impact effect of the concrete materials (P). The above intelligent techniques as used in predicting Fc28 were also used, and the outcome showed that EPR with a perfect coefficient of determination outclassed the other techniques in the following order: GP-0.999, ANN-GRG-0.999, and ANN-BP-0.994. This time, EPR was adjudged the decisive technique for predicting life cycle assessment and the environmental impact potential of utilizing the concrete constituents. Finally, FA was adjudged to have a 62% degree of importance which, being a good degree above average, could replace cement.

$$\begin{aligned} Fc28 = {} & \frac{929\ W - 60\ FAg - 178\ FA - 194{,}750}{C} \\ & + \frac{57\ FA + 161\ FAg - 148\ CAg}{W} + \frac{583\ C - 912{,}613}{FAg} \\ & - \frac{12.7\ C}{FA} - \frac{40\ C}{CAg} + \frac{22{,}200{,}000}{W.C} + \frac{1{,}200{,}000}{W.FA} \\ & + \frac{34{,}000{,}000}{W.FAg} - \frac{197{,}000{,}000}{W.CAg} - \frac{737{,}787}{C.FA} \\ & - \frac{14{,}000{,}000}{C.FAg} + \frac{363{,}000{,}000}{FAg.CAg} + \frac{FAg.CAg}{171} + \frac{W.CAg}{217} \\ & - \frac{C.FA}{220} - \frac{C.FAg}{574} - \frac{C.CAg}{231} - \frac{C^2}{256} + \frac{W^2}{86} - 21\ W \\ & + 3.8\ C + 6856 \end{aligned} \tag{5}$$

$$P = 0.24 + \frac{C}{58.5} + \frac{FA}{51} \tag{6}$$

4. Conclusions

This research presents three models using five AI techniques (GP, ANN-BP, ANN-GRG, ANN-GA, and EPR) to predict both 28-day compressive strength (Fc28) and the environmental impact factor (P) of FA-based concrete using water content (W), cement content (C), fly ash content (FA), fine aggregate (sand) content (FAg) and coarse aggregate content (CAg) as the independent variables of the concrete mixes. First, it can be remarked that the concrete mixes with a higher amount of cement than FA showed higher compressive strength and environmental impact, while those with a higher amount of FA showed relatively lower strength and environmental impact. Meanwhile, the closed-form equations and the proposed models present optimization models with which the optimal amount of FA needed to achieve optimal strength and minimal environmental impact can be determined prior to the design and production of concrete. This agrees with previous research works on the utilization of high-volume fly ash in concrete [75–81]. The results of comparing the accuracies of the developed models can be concluded in the following points:

- Regarding Fc28, the GP model was the simplest and the least accurate one (80.9%). Then, EPR had an accuracy of 89.9%, and finally the three ANN models had almost the same accuracy of ≈94.0%;
- Regarding P, all five models had almost the same accuracy (99.0%);
- The prediction accuracy of the EPR model was lower than the ANN models, but their outputs were closed-form equations that could be used manually or as software, unlike the ANN output, which cannot be used manually;
- The results indicate that the accuracy of the ANN model was slightly affected by the training algorithm. The back propagation (BP) showed the best level of accuracy (94.9% and 97.8%), gradually reduced gradient (GRG) came in the second with accuracies of

94.2% and 99.2%, and the genetic algorithm (GA) showed the lowest level of accuracy with 93.0% and 99.0% for Fc28 and P, respectively;
- The summation of the absolute weights of each neuron in the input layer of the developed ANN model indicated that for both Fc28 and P, cement content (C) was the most important factor, and then aggregate content (FAg and CAg). Fly ash and water content came last in the importance ranking;
- Both the GP and EPR models indicated that the environmental impact factor (P) depended only on the cementitious materials (C and FA);
- The GA technique successfully reduced the 56 and 6 terms of conventional polynomial regression quadrilateral formula to only 28 and 3 terms for Fc28 and P, respectively, without a significant impact on accuracy;
- Similar to any other regression technique, the generated formulas were valid within the considered range of parameter values; beyond this range, the prediction accuracy should be verified.

Author Contributions: Conceptualization, K.C.O. and D.-P.N.K.; methodology, K.C.O. and D.-P.N.K.; software, K.C.O., D.-P.N.K. and A.M.E.; validation, K.C.O. and D.-P.N.K.; formal analysis, K.C.O. and D.-P.N.K.; investigation, K.C.O. and D.-P.N.K.; resources, K.C.O. and D.-P.N.K.; data curation, K.C.O. and D.-P.N.K.; writing—original draft preparation, K.C.O., D.-P.N.K., A.M.E., F.D., A.S., H.J. and M.L.N.; writing—review and editing, K.C.O., D.-P.N.K. and M.L.N.; visualization, K.C.O. and D.-P.N.K.; supervision, K.C.O. and D.-P.N.K.; project administration, K.C.O. and D.-P.N.K. All authors have read and agreed to the published version of the manuscript.

Funding: This research received no external funding.

Institutional Review Board Statement: Not applicable.

Informed Consent Statement: Not applicable.

Data Availability Statement: The data supporting the results has been reported within the article.

Conflicts of Interest: The authors declare no conflict of interest.

References

1. Malhotra, V. Introduction: Sustainable Development and Concrete Technology. *Concr. Int.* **2002**, *24*, 22.
2. Dabbaghi, F.; Rashidi, M.; Nehdi, M.L.; Sadeghi, H.; Karimaei, M.; Rasekh, H.; Qaderi, F. Experimental and Informational Modeling Study on Flexural Strength of Eco-Friendly Concrete Incorporating Coal Waste. *Sustain.* **2021**, *13*, 7506. [CrossRef]
3. Kafi, M.A.; Sadeghi-Nik, A.; Bahari, A.; Sadeghi-Nik, A.; Mirshafiei, E. Microstructural Characterization and Mechanical Properties of Cementitious Mortar Containing Montmorillonite Nanoparticles. *J. Mater. Civ. Eng.* **2016**, *28*, 04016155. [CrossRef]
4. Sadeghi-Nik, A.; Lotfi-Omran, O.; Khalilpasha, M.H.; Nik, A.S.; Omran, O.L.; Kimiaeifard, K.; Molla, M.A. Properties of Lime-Cement Concrete Containing Various Amounts of Waste Tire Powder under Different Ground Moisture Conditions. *Adv. Civ. Archit. Constr. Eng. Manag.* **2022**, *14*, 482. [CrossRef]
5. Dabbaghi, F.; Fallahnezhad, H.; Nasrollahpour, S.; Dehestani, M.; Yousefpour, H. Evaluation of Fracture Energy, Toughness, Brittleness, and Fracture Process Zone Properties for Lightweight Concrete Exposed to High Temperatures. *Theor. Appl. Fract. Mech.* **2021**, *116*, 103088. [CrossRef]
6. Amiri, H.; Azadi, S.; Karimaei, M.; Sadeghi, H. Farshad Dabbaghi Multi-Objective Optimization of Coal Waste Recycling in Concrete Using Response Surface Methodology. *J. Build. Eng.* **2022**, *45*, 103472. [CrossRef]
7. Dabbaghi, F.; Sadeghi-Nik, A.; Ali Libre, N.; Nasrollahpour, S. Characterizing Fiber Reinforced Concrete Incorporating Zeolite and Metakaolin as Natural Pozzolans. *Structures* **2021**, *34*, 2617–2627. [CrossRef]
8. Bahari, A.; Sadeghi-Nik, A.; Roodbari, M.; Sadeghi-Nik, A.; Mirshafiei, E. Experimental and Theoretical Studies of Ordinary Portland Cement Composites Contains Nano LSCO Perovskite with Fokker-Planck and Chemical Reaction Equations. *Constr. Build. Mater.* **2018**, *163*, 247–255. [CrossRef]
9. Bahari, A.; Sadeghi-Nik, A.; Shaikh, F.U.A.; Sadeghi-Nik, A.; Cerro-Prada, E.; Mirshafiei, E.; Roodbari, M. Experimental Studies on Rheological, Mechanical, and Microstructure Properties of self-compacting Concrete Containing Perovskite Nanomaterial. *Struct. Concr.* **2021**, *23*, 564–578. [CrossRef]
10. Ahmaruzzaman, M. A Review on the Utilization of Fly Ash. *Prog. Energy Combust. Sci.* **2010**, *36*, 327–363. [CrossRef]
11. Sadeghi-Nik, A.; Berenjian, J.; Bahari, A.; Safaei, A.S.; Dehestani, M. Modification of Microstructure and Mechanical Properties of Cement by Nanoparticles through a Sustainable Development Approach. *Constr. Build. Mater.* **2017**, *155*, 880–891. [CrossRef]
12. Bahari, A.; Berenjian, J.; Sadeghi-Nik, A. Modification of Portland Cement with Nano SiC. *Proc. Natl. Acad. Sci. India Sect. A Phys. Sci.* **2016**, *86*, 323–331. [CrossRef]

13. Nonavinakere, S.; Reed, B.E. Fly Ash Enhanced Metal Removal Process. In Proceedings of the Mid-Atlantic Industrial Waste Conference, Bethlehem, PA, USA, 31 December 1995.
14. González, A.; Navia, R.; Moreno, N. Fly Ashes from Coal and Petroleum Coke Combustion: Current and Innovative Potential Applications. *Waste Manag. Res.* **2009**, *27*, 976–987. [CrossRef] [PubMed]
15. Juenger, M.C.G.; Siddique, R. Recent Advances in Understanding the Role of Supplementary Cementitious Materials in Concrete. *Cem. Concr. Res.* **2015**, *78*, 71–80. [CrossRef]
16. Rashidi, M.; Joshaghani, A.; Ghodrat, M. Towards Eco-Flowable Concrete Production. *Sustainability* **2020**, *12*, 1208. [CrossRef]
17. Saha, A.K.; Sarker, P.K. Sustainable Use of Ferronickel Slag Fine Aggregate and Fly Ash in Structural Concrete: Mechanical Properties and Leaching Study. *J. Clean. Prod.* **2017**, *162*, 438–448. [CrossRef]
18. Berndt, M.L. Properties of Sustainable Concrete Containing Fly Ash, Slag and Recycled Concrete Aggregate. *Constr. Build. Mater.* **2009**, *23*, 2606–2613. [CrossRef]
19. Pellegrino, C.; Gaddo, V. Mechanical and Durability Characteristics of Concrete Containing EAF Slag as Aggregate. *Cem. Concr. Compos.* **2009**, *31*, 663–671. [CrossRef]
20. Li, G.; Zhao, X. Properties of Concrete Incorporating Fly Ash and Ground Granulated Blast-Furnace Slag. *Cem. Concr. Compos.* **2003**, *25*, 293–299. [CrossRef]
21. ACI Committee 211.1-91. Standard Practice for Selecting Proportions for Normal, Heavyweight, and Mass Concrete. In *ACI Manual of Concrete Practice: Part 1*; American Concrete Institute: Farming Hills, MI, USA, 2000; Volume 38.
22. Chindaprasirt, P.; Jaturapitakkul, C.; Chalee, W.; Rattanasak, U. Comparative study on the characteristics of fly ash and bottom ash geopolymers. *Waste Manag.* **2009**, *29*, 539–543. [CrossRef]
23. Chindaprasirt, P.; Chotithanorm, C.; Cao, H.T.; Sirivivatnanon, V. Influence of Fly Ash Fineness on the Chloride Penetration of Concrete. *Constr. Build. Mater.* **2007**, *2*, 356–361. [CrossRef]
24. Atiş, C.D.D. High-Volume Fly Ash Concrete with High Strength and Low Drying Shrinkage. *J. Mater. Civ. Eng.* **2003**, *15*, 153–156. [CrossRef]
25. Supit, S.W.M.; Shaikh, F.U.A. Durability Properties of High Volume Fly Ash Concrete Containing Nano-Silica. *Mater. Struct.* **2014**, *48*, 2431–2445. [CrossRef]
26. Ravina, D.; Mehta, P.K. Properties of Fresh Concrete Containing Large Amounts of Fly Ash. *Cem. Concr. Res.* **1986**, *16*, 227–238. [CrossRef]
27. Mardani-Aghabaglou, A.; Andiç-Çakir, Ö.; Ramyar, K. Freeze–Thaw Resistance and Transport Properties of High-Volume Fly Ash Roller Compacted Concrete Designed by Maximum Density Method. *Cem. Concr. Compos.* **2013**, *37*, 259–266. [CrossRef]
28. Gopalan, M.K. Sorptivity of Fly Ash Concretes. *Cem. Concr. Res.* **1996**, *26*, 1189–1197. [CrossRef]
29. Haque, M.N.; Kayali, O. Properties of High-Strength Concrete Using a Fine Fly Ash. *Cem. Concr. Res.* **1998**, *28*, 1445–1452. [CrossRef]
30. Sumer, M. Compressive Strength and Sulfate Resistance Properties of Concretes Containing Class F and Class C Fly Ashes. *Constr. Build. Mater.* **2012**, *34*, 531–536. [CrossRef]
31. Siddique, R. Performance Characteristics of High-Volume Class F Fly Ash Concrete. *Cem. Concr. Res.* **2004**, *34*, 487–493. [CrossRef]
32. Supit, S.W.; Shaikh, F.U.; Sarker, P.K. Effect of ultrafine fly ash on mechanical properties of high volume fly ash mortar. *Constr Build Mater.* **2014**, *51*, 278–286. [CrossRef]
33. Ahn, Y.B.; Jang, J.G.; Lee, H.K. Mechanical Properties of Lightweight Concrete Made with Coal Ashes after Exposure to Elevated Temperatures. *Cem. Concr. Compos.* **2016**, *72*, 27–38. [CrossRef]
34. Wang, S.; Llamazos, E.; Baxter, L.; Fonseca, F. Durability of Biomass Fly Ash Concrete: Freezing and Thawing and Rapid Chloride Permeability Tests. *Fuel* **2008**, *87*, 359–364. [CrossRef]
35. Naik, T.R.; Singh, S.; Ramme, B. Mechanical Properties and Durability of Concrete Made with Blended Fly Ash. *Mater. J.* **1998**, *95*, 454–462. [CrossRef]
36. Malhotra, V.M. Durability of Concrete Incorporating High-Volume of Low-Calcium (ASTM Class F) Fly Ash. *Cem. Concr. Compos.* **1990**, *12*, 271–277. [CrossRef]
37. Kate, G.K.; Nayak, C.B.; Thakare, S.B. Optimization of Sustainable High-Strength–High-Volume Fly Ash Concrete with and without Steel Fiber Using Taguchi Method and Multi-Regression Analysis. *Innov. Infrastruct. Solut.* **2021**, *6*, 102. [CrossRef]
38. Naseri, H.; Jahanbakhsh, H.; Khezri, K.; Shirzadi Javid, A.A. Toward Sustainability in Optimizing the Fly Ash Concrete Mixture Ingredients by Introducing a New Prediction Algorithm. *Environ. Dev. Sustain.* **2021**, *24*, 2767–2803. [CrossRef]
39. International Organization for Standardization. *Environmental Management—Life Cycle Assessment—Principles and Framework*; ISO: Geneva, Switzerland, 2006.
40. Dabbaghi, F.; Nasrollahpour, S.; Dehestani, M.; Yousefpour, H. Optimization of Concrete Mixtures Containing Lightweight Expanded Clay Aggregates Based on Mechanical, Economical, Fire-Resistance, and Environmental Considerations. *J. Mater. Civ. Eng.* **2021**, *34*, 04021445. [CrossRef]
41. Celik, K.; Meral, C.; Petek Gursel, A.; Mehta, P.K.; Horvath, A.; Monteiro, P.J.M. Mechanical Properties, Durability, and Life-Cycle Assessment of Self-Consolidating Concrete Mixtures Made with Blended Portland Cements Containing Fly Ash and Limestone Powder. *Cem. Concr. Compos.* **2015**, *56*, 59–72. [CrossRef]
42. Huntzinger, D.N.; Eatmon, T.D. A Life-Cycle Assessment of Portland Cement Manufacturing: Comparing the Traditional Process with Alternative Technologies. *J. Clean. Prod.* **2009**, *17*, 668–675. [CrossRef]

43. Chen, C.; Habert, G.; Bouzidi, Y.; Jullien, A.; Ventura, A. LCA Allocation Procedure Used as an Incitative Method for Waste Recycling: An Application to Mineral Additions in Concrete. *Resour. Conserv. Recycl.* **2010**, *54*, 1231–1240. [CrossRef]
44. Collins, F. Inclusion of Carbonation during the Life Cycle of Built and Recycled Concrete: Influence on Their Carbon Footprint. *Int. J. Life Cycle Assess.* **2010**, *15*, 549–556. [CrossRef]
45. García-Segura, T.; Yepes, V.; Alcalá, J. Life Cycle Greenhouse Gas Emissions of Blended Cement Concrete Including Carbonation and Durability. *Int. J. Life Cycle Assess.* **2014**, *19*, 3–12. [CrossRef]
46. Shi, C.; Jiménez, A.F.; Palomo, A. New Cements for the 21st Century: The Pursuit of an Alternative to Portland Cement. *Cem. Concr. Res.* **2011**, *7*, 750–763. [CrossRef]
47. O'Brien, K.R.; Ménaché, J.; O'Moore, L.M. Impact of Fly Ash Content and Fly Ash Transportation Distance on Embodied Greenhouse Gas Emissions and Water Consumption in Concrete. *Int. J. Life Cycle Assess.* **2009**, *7*, 621–629. [CrossRef]
48. Iftikhar, B.; Alih, S.C.; Vafaei, M.; Elkotb, M.A.; Shutaywi, M.; Javed, M.F.; Deebani, W.; Khan, M.I.; Aslam, F. Predictive Modeling of Compressive Strength of Sustainable Rice Husk Ash Concrete: Ensemble Learner Optimization and Comparison. *J. Clean. Prod.* **2022**, *348*, 131285. [CrossRef]
49. Pradhan, S.; Chang Boon Poh, A.; Qian, S. Impact of Service Life and System Boundaries on Life Cycle Assessment of Sustainable Concrete Mixes. *J. Clean. Prod.* **2022**, *342*, 130847. [CrossRef]
50. Rehan, R.; Nehdi, M. Carbon Dioxide Emissions and Climate Change: Policy Implications for the Cement Industry. *Environ. Sci. Policy* **2005**, *8*, 105–114. [CrossRef]
51. Liu, Z.; Takasu, K.; Koyamada, H.; Suyama, H. A Study on Engineering Properties and Environmental Impact of Sustainable Concrete with Fly Ash or GGBS. *Constr. Build. Mater.* **2022**, *316*, 125776. [CrossRef]
52. Colaço, R. Reduce the Environmental Impact of Cement. *Constr. Mag.* **2019**, *90*, 12–14.
53. Rahla, K.M.; Mateus, R.; Bragança, L. Comparative Sustainability Assessment of Binary Blended Concretes Using Supplementary Cementitious Materials (SCMs) and Ordinary Portland Cement (OPC). *J. Clean. Prod.* **2019**, *220*, 445–459. [CrossRef]
54. Schorcht, F.; Kourti, I.; Scalet, B.M.; Roudier, S.; Sancho, L.D. *Best Available Techniques (BAT) Reference Document for the Production of Cement, Lime and Magnesium Oxide*; European Commission Joint Research Centre Institute for Prospective Technological Studies: Luxembourg, 2013.
55. Supino, S.; Malandrino, O.; Testa, M.; Sica, D. Sustainability in the EU Cement Industry: The Italian and German Experiences. *J. Clean. Prod.* **2016**, *112*, 430–442. [CrossRef]
56. Tang, P.; Chen, W.; Xuan, D.; Zuo, Y.; Poon, C.S. Investigation of Cementitious Properties of Different Constituents in Municipal Solid Waste Incineration Bottom Ash as Supplementary Cementitious Materials. *J. Clean. Prod.* **2020**, *258*, 120675. [CrossRef]
57. He, Z.-H.; Zhu, H.-N.; Zhang, M.-Y.; Shi, J.-Y.; Du, S.-G.; Liu, B. Autogenous Shrinkage and Nano-Mechanical Properties of UHPC Containing Waste Brick Powder Derived from Construction and Demolition Waste. *Constr. Build. Mater.* **2021**, *306*, 124869. [CrossRef]
58. Aprianti, S.E. A Huge Number of Artificial Waste Material Can Be Supplementary Cementitious Material (SCM) for Concrete Production—A Review Part II. *J. Clean. Prod.* **2017**, *142*, 4178–4194. [CrossRef]
59. Wang, N.; Sun, X.; Zhao, Q.; Yang, Y.; Wang, P. Leachability and Adverse Effects of Coal Fly Ash: A Review. *J. Hazard. Mater.* **2020**, *396*, 122725. [CrossRef]
60. Heidrich, C.; Feuerborn, H.; Weir, A. Coal Combustion Products: A Global Perspective. In Proceedings of the World of Coal Ash (WOCA) Conference, Lexington, KY, USA, 22 April 2013.
61. National Development and Reform Commission. *Annual Report on Comprehensive Utilization of Resources in China*; National Development and Reform Commission: Beijing, China, 2014.
62. Central Electricity Authority. *Report On, Fly Ash Generation at Coal/Lignite Based Thermal Power Stations and its Utilization in the Country for The Year 2014–2015*; Central Electricity Authority (CEA): New Delhi, India, 2016.
63. American Coal Ash Association. *2013 Coal Combustion Product (CCP) Production & Use Survey Report*; American Coal Ash Association (ACAA): Farmington Hills, MI, USA, 2013.
64. Neville, A.M. *Properties of Concrete*; Longman: London, UK, 1995; Volume 4.
65. Rafieizonooz, M.; Khankhaje, E.; Rezania, S. Assessment of Environmental and Chemical Properties of Coal Ashes Including Fly Ash and Bottom Ash, and Coal Ash Concrete. *J. Build. Eng.* **2022**, *49*, 104040. [CrossRef]
66. Chindaprasirt, P.; Jaturapitakkul, C.; Sinsiri, T. Effect of fly ash fineness on compressive strength and pore size of blended cement paste. *Cem. Concr. Compos.* **2005**, *27*, 425–428. [CrossRef]
67. Moffatt, E.G.; Thomas, M.D.A.; Fahim, A. Performance of High-Volume Fly Ash Concrete in Marine Environment. *Cem. Concr. Res.* **2017**, *102*, 127–135. [CrossRef]
68. Hussain, S.; Bhunia, D.; Singh, S.B. Comparative Study of Accelerated Carbonation of Plain Cement and Fly-Ash Concrete. *J. Build. Eng.* **2017**, *10*, 26–31. [CrossRef]
69. Hefni, Y.; El Zaher, Y.A.; Wahab, M.A. Influence of Activation of Fly Ash on the Mechanical Properties of Concrete. *Constr. Build. Mater.* **2018**, *172*, 728–734. [CrossRef]
70. Kara De Maeijer, P.; Craeye, B.; Snellings, R.; Kazemi-Kamyab, H.; Loots, M.; Janssens, K.; Nuyts, G. Effect of Ultra-Fine Fly Ash on Concrete Performance and Durability. *Constr. Build. Mater.* **2020**, *263*, 120493. [CrossRef]
71. Garg, C.; Namdeo, A.; Singhal, A.; Singh, P.; Shaw, R.N.N.; Ghosh, A. *Adaptive Fuzzy Logic Models for the Prediction of Compressive Strength of Sustainable Concrete*; Springer: Singapore, 2022; pp. 593–605.

72. Zhao, H.; Sun, W.; Wu, X.; Gao, B. Sustainable Self-Compacting Concrete Containing High-Amount Industrial by-Product Fly Ash as Supplementary Cementitious Materials. *Environ. Sci. Pollut. Res.* **2022**, *29*, 3616–3628. [CrossRef] [PubMed]
73. Khursheed, S.; Jagan, J.; Samui, P.; Kumar, S. Compressive Strength Prediction of Fly Ash Concrete by Using Machine Learning Techniques. *Innov. Infrastruct. Solut.* **2021**, *6*, 149. [CrossRef]
74. Hansen, T.C. Long-Term Strength of High Fly Ash Concretes. *Cem. Concr. Res.* **1990**, *20*, 193–196. [CrossRef]
75. Mehta, P.K.; Gjørv, O.E. Properties of Portland Cement Concrete Containing Fly Ash and Condensed Silica-Fume. *Cem. Concr. Res.* **1982**, *12*, 587–595. [CrossRef]
76. Ravina, D.; Mehta, P.K. Compressive Strength of Low Cement/High Fly Ash Concrete. *Cem. Concr. Res.* **1988**, *18*, 571–583. [CrossRef]
77. Thomas, M.D.A.; Matthews, J.D. Carbonation of Fly Ash Concrete. *Mag. Concr. Res.* **1992**, *44*, 217–228. [CrossRef]
78. Lam, L.; Wong, Y.L.; Poon, C.S. Effect of Fly Ash and Silica Fume on Compressive and Fracture Behaviors of Concrete. *Cem. Concr. Res.* **1998**, *28*, 271–283. [CrossRef]
79. Atiş, C.D. Heat Evolution of High-Volume Fly Ash Concrete. *Cem. Concr. Res.* **2002**, *32*, 751–756. [CrossRef]
80. Oner, A.; Akyuz, S.; Yildiz, R. An Experimental Study on Strength Development of Concrete Containing Fly Ash and Optimum Usage of Fly Ash in Concrete. *Cem. Concr. Res.* **2005**, *35*, 1165–1171. [CrossRef]
81. Chalee, W.; Ausapanit, P.; Jaturapitakkul, C. Utilization of Fly Ash Concrete in Marine Environment for Long Term Design Life Analysis. *Mater. Des.* **2010**, *31*, 1242–1249. [CrossRef]
82. Liu, M.H.; Wang, Y.F. Prediction of the Strength Development of Fly Ash Concrete. *Adv. Mater. Res.* **2010**, *150–151*, 1026–1033. [CrossRef]
83. Pitroda, D.J. Prediction of Strength for Fly Ash Cement Concrete through Soft Computing Approaches. *Int. J. Adv. Res. Eng. Sci. Manag.* **2020**, *1*, 1766–2394.
84. Chopra, P.; Sharma, R.K.; Kumar, M. Prediction of Compressive Strength of Concrete Using Artificial Neural Network and Genetic Programming. *Adv. Mater. Sci. Eng.* **2016**, *2016*, 7648467. [CrossRef]
85. Ebid, A.M. 35 Years of (AI) in Geotechnical Engineering: State of the Art. *Geotech. Geol. Eng.* **2021**, *39*, 637–690. [CrossRef]